Article:
Thakur, R, Laye, JP, Lauss, M et al. (2019) Transcriptomic Analysis Reveals Prognostic Molecular Signatures of Stage I Melanoma. Clinical Cancer Research, 25 (24). pp. 7424-7435. ISSN: 1078-0432

https://doi.org/10.1158/1078-0432.CCR-18-3659

Transcriptomic classification of primary melanoma reveals molecular signatures which add prognostic value to current staging systems including stage I disease

Rohit Thakur[1,2], Jonathan P. Laye[1], Martin Lauss[3], Joey Mark S. Diaz[1], Sally Jane O'Shea[4,5], Joanna Poźniak[1,6,7], Anastasia Filia[8], Mark Harland[1], Joanne Gascoyne[1], Juliette A. Randerson-Moor[1], May Chan[1], Tracey Mell[1], Göran Jönsson[3], D. Timothy Bishop[1], Julia Newton-Bishop[1,$], Jennifer H. Barrett[1,$] and Jérémie Nsengimana[1,$,*]

[1]University of Leeds School of Medicine, Leeds, LS97TF, United Kingdom

[2]Department of Surgical Oncology, MD Anderson Cancer Center, Houston, TX, USA, 77054

[3]Division of Oncology and Pathology, Department of Clinical Sciences Lund, Faculty of Medicine, Lund University, Lund, 22381, Sweden

[4]Mater Private Hospital Cork, Mahon, Cork, T12 K199, Ireland

[5]School of Medicine, University College Cork, College Road, Cork, T12 AK54, Ireland

[6]Laboratory for Molecular Cancer Biology, VIB Center for Cancer Biology, KU Leuven, Leuven, Belgium

[7]Department of Oncology, KU Leuven, Leuven, Belgium

[8] Centre for Translational Research, Biomedical Research Foundation of the Academy of Athens (BRFAA), Athens, Greece

Running title: Prognostic gene signature in stage I melanoma

Keywords: Consensus clustering, Sentinel Node Biopsy, EMT, *JUN*, *AXL*

The authors have declared no conflicts of interest.

[$] These authors contributed equally to the work

*Correspondence: Dr Jérémie Nsengimana, Saint James University Hospital, Clinical Sciences Building room 6.6, Beckett Street, Leeds, LS9 7TF, United Kingdom, J.Nsengimana@leeds.ac.uk, Phone: +44 113 2068974

This work was funded by Cancer Research UK C588/A19167, C8216/A6129, and C588/A10721 and NIH CA83115. RT, JMSD and JP are supported by Horizon 2020 Research and Innovation Programme no. 641458 (MELGEN). Copy number data were generated using AICR grant 12-0023.

Total number of words (Introduction, Methods, Results and Discussion): 4120

Abstract: 245 words

Total number of figures: 5

Total number of tables: 1

Supplementary files: 2

Translational relevance:

The introduction of adjuvant but toxic therapies for primary melanoma has highlighted the need to stratify patients based on improved prognostic and predictive biomarkers. We report a six-class transcriptomic signature generated from primary melanomas which predicted prognosis, notably in stage I disease. The signature demonstrated comparable prognostic value to that of sentinel node biopsy. When the six classes were applied to published transcriptomic datasets from patients treated with immunotherapy, one class consistently predicted poor outcome. This class was characterised by expression of *JUN* and *AXL*, both known determinants of poor therapeutic response in advanced melanoma. These findings suggest that the six-class signature should be applied to larger datasets as they become available, in order to further validate its clinical relevance as a prognostic/predictive biomarker in the adjuvant setting.

Abstract

Background

Previously identified transcriptomic signatures have been based on primary and metastatic melanomas with relatively few AJCC stage I tumors given difficulties in sampling small tumors. The advent of adjuvant therapies has highlighted the need for better prognostic and predictive biomarkers especially for AJCC stage I and II disease.

Patients and Methods

687 primary melanoma transcriptomes were generated from the Leeds Melanoma Cohort (LMC). The prognostic value of existing signatures across all the AJCC stages was tested. Unsupervised clustering was performed and the prognostic value of the resultant signature was compared with that of sentinel node biopsy (SNB) and tested as a biomarker in three published immunotherapy datasets.

Results

Previous Lund and TCGA signatures predicted outcome in the LMC dataset (P=10^{-8} to 10^{-4}) but showed a significant interaction with AJCC stage (P=0.04) and did not predict outcome in stage I tumors (P=0.3 to 0.7). Consensus-based classification of the LMC dataset identified six classes which predicted outcome, notably in stage I disease. LMC class was a similar indicator of prognosis when compared to SNB and it added prognostic value to the genes reported by Gerami *et al*. One particular LMC class consistently predicted poor outcome in patients receiving immunotherapy in two of three tested datasets. Biological characterisation of this class revealed high *JUN* and *AXL* expression and evidence of epithelial to mesenchymal transition.

Conclusion

A transcriptomic signature of primary melanoma was identified with prognostic value, including in stage I melanoma and in patients undergoing immunotherapy.

Introduction

Cutaneous melanoma continues to increase in incidence worldwide. Although earlier diagnosis has been documented with correspondingly better outcomes, the rising incidence of thinner tumors means that, counterintuitively, one fifth of deaths now occur in patients presenting initially with early disease (1). In the UK, 91% of melanomas are diagnosed at AJCC stage I to II (2). Therefore, better prognostic biomarkers are needed to identify early stage disease requiring adjuvant therapies, as well as predictive biomarkers of response to checkpoint blockade.

Previous transcriptomic analyses of cutaneous melanoma have generated gene signatures with a prognostic value independent of AJCC stage (3-7). The prognostic signature developed by Jonsson *et al.* (3) classifies metastatic melanomas into four classes (*Lund 4-classes*), later simplified into two classes (*Lund 2-grades*, (4)), and the signature developed by the TCGA (The Cancer Genome Atlas) consortium classified melanomas into three classes (*TCGA 3-classes*) (8). The prognostic significance of the Lund 4-class and TCGA 3-class signatures have been replicated in relatively small datasets, notably with few AJCC stage I patients (5,9). Another transcriptomic signature based on 27 genes was developed by Gerami *et al.* (6) to classify primary melanoma patients into tumors which were high or low-risk for metastasis.

In this study, the first aim was to test the prognostic value of the Lund and TCGA signatures, as well as the gene list of Gerami et al's signature (6) in a large population-based cohort of primary melanomas with a good proportion of stage I patients and extensive phenotypic annotations (Leeds Melanoma Cohort, LMC). Since the dataset was well powered for discovery of novel tumor subtypes, unsupervised clustering of the tumor transcriptomes of the LMC was performed and the prognostic value of the resultant signature was compared with that of SNB in analyses stratified by AJCC stage. Finally, the association between the Leeds signature and outcome was tested in published data from patients receiving immunotherapy (10-12).

Materials and Methods

Leeds Melanoma Cohort

As described previously (13), 2184 primary melanoma patients were recruited to the Leeds Melanoma Cohort (LMC) in the period of 2000-2012. This was a population-ascertained cohort which therefore recruited patients treated at multiple clinical centres (recruitment rate 67%). During this period SNB was neither offered nor accepted universally. The study was ethically approved (ethical approval MREC 1/3/57, PIAG 3-09(d)/2003) and in accordance with the Declaration of Helsinki. Participants were consented to sampling of their FFPE (formalin fixed paraffin embedded) tumor blocks which were stored in the NHS (UK National Health Service) histopathology departments of the respective hospitals. Haemotoxylin and eosin (H&E)-stained slides were generated and examined to facilitate subsequent sampling of the blocks using a 0.6mm diameter tissue microarray needle as previously reported (5,13). Prior to sampling, all the tumor blocks were reviewed, and if there was only a small amount of tumor left in the block then the block was not sampled, lest a clinically important block be destroyed. Up to two cores were sampled from each block, and, to increase the comparability between tumors, the samples were consistently extracted from the least inflamed, least stromal regions of the invasive front of the tumor. The tumor infiltrating lymphocytes were scored using Clark *et al.'s* classification system (14). As previously reported (13), 703 tumor transcriptomes were profiled and in the current study 16 samples were removed in quality control leaving a cohort of 687 patients, henceforth referred to as the whole LMC dataset. The dataset contained 251 patients who had a SNB test (Supplementary table S10), and only 16 patients are known so far to have been treated with checkpoint blockade. The LMC patients were assigned an AJCC stage based on the AJCC staging 8th edition (15). Where patients did not have a SNB, the AJCC staging used was derived from clinical staging and pathological examination of the wide local excision sample.

mRNA extraction and expression data generation

Both mRNA and DNA were extracted from the tumor samples derived from cores following a previously described protocol (5,13). The whole genome mRNA expression profiling was carried out using Illumina's DASL-HT12-v4 array. As described previously, for quality control, the mRNA was

extracted from up to 2 cores for a number of patients (117 duplicates in total); gene expression data from only one extraction per patient was used in subsequent analyses (13). The raw transcriptomic data were extracted from the image files using GenomeStudio (Illumina Inc., San Diego) and were pre-processed as previously reported (13). Briefly, after background correction and quantile normalisation (R package *LUMI* (16)), singular value decomposition (SVD) was used to remove the batch effect (R package *SWAMP* (17)) (13).

Quality control in LMC

The array included 29,262 probes corresponding to 20,715 unique genes. For genes with multiple probes, the probe detected in the largest number of tumors was retained, and two additional filters were applied: genes had to be detected with $P<0.05$ in at least 40% of tumors and had to have a standard deviation (SD)>0.40. This SD threshold was chosen based on the overall distribution across the 20,715 genes on the log2 scale. The median SD was 0.68. The data were standardized to give each gene a mean of 0 and SD of 1.

Procedures

The LMC tumors were classified into the Lund 4-classes, Lund 2-grades and TCGA 3-classes using the supervised nearest centroid classification (NCC) as previously described (5). All the 27 genes of the Gerami *et al.* gene signature (6) were present in LMC dataset and were analysed using a univariable survival analysis in the whole LMC dataset and stage I tumors. Unsupervised clustering was performed using the consensus Partitioning Around Medoids clustering method in the R-package *ConsensusClusterPlus* (18,19) with Euclidean distance as the dissimilarity measure and a resampling fraction of 0.8 for both genes and samples in 1000 iterations (Supplementary methods).

Statistical analysis

Cox proportional hazard models and Kaplan-Meier curves were used to test the association with survival (R-package *Survival*) (20). The survival time was calculated from time of diagnosis to time of last follow-up or time of death from melanoma, whichever occurred first, referred to as melanoma-specific survival (MSS). Patients with deaths caused by factors other than melanoma were censored at the time of death. Receiver Operating Characteristic (ROC) analysis was performed using AJCC

stage pre-SNB and AJCC stage post-SNB for patients who had SNB. Clinical staging prior to SNB is described as AJCC pre-SNB. The AJCC stage post-SNB includes additional information on regional lymph node metastasis. The analysis used AJCC staging 8th edition, and MSS up to 3 years was chosen as cut-off based upon the inclusion of the majority of the deaths without loss of data as a result of censoring (Supplementary table S11). Patients who were censored before 3 years were not included in the analysis. The analysis was performed using R-packages *pROC*, *plotROC,* and *ggplot2* (21-23).

Pathway enrichment analysis

The differentially expressed genes (DEG) were identified using the Significance Analysis of Microarrays (R-package *SAMR*) by comparing each class versus all others (24). Pathway enrichment and biological network analysis of DEGs with a q-value equal to 0 were performed using ReactomeFiviz in Cytoscape (25). The central nodes of the biological network were identified using a centrality measure (betweenness) in *Gephi* (26) (Supplementary methods).

Copy Number Alterations (CNA)

The CNA data were generated in a subset of LMC tumors using Illumina's next-generation sequencing platform as reported in Filia *et al.* (in revision) (Supplementary methods). Among the 687 transcriptome-profiled patients of LMC, CNA data were available for 272 patients. The CNA were assessed in the regions spanning the genes identified as hubs in network enrichment analysis. The ratio between mean of the window read counts in the region mapping to a gene and the average read count of the 10 flanking regions around that gene was used to estimate the copy number changes. The windows (5k) corresponding to a gene locus were identified using the R packages *biomaRt* (27,28). The cut-off for calling a region amplified was chosen as a value greater than 0.4 while a value less than -0.4 was used to identify a deletion. The 272 samples in the CNA dataset were at AJCC stages I (n=80), II (n=147), and III (n=45) (similar distribution to the whole LMC dataset).

Lund validation dataset

For replication, a primary melanoma transcriptomic dataset of 223 tumors from a Lund cohort (Sweden) was used (Harbst *et al.* (4)). The samples were classified using the newly generated signature by the supervised NCC approach (5). Out of those 223 patients, 200 had recorded

information on melanoma relapse in the follow-up time post-diagnosis and were used to test the association between patient subgroups and relapse-free survival (using Cox proportional hazard models, Kaplan-Meier curves and log-rank test).

Immunotherapy datasets

Three publicly available transcriptome datasets (Hugo Cohort: GSE78220, Ulloa-Monotoya cohort: GSE35640, Riaz Cohort: https://github.com/riazn/bms038_analysis) were downloaded (10-12), samples were quantile normalised and classified using the NCC method (Pearson's correlation coefficient). The Riaz cohort was a mixture of samples from various melanoma types (cutaneous melanoma, mucosal melanoma, acral melanoma, uveal/ocular melanoma, others). In this study the samples labelled as cutaneous melanoma were analysed. In all the three cohorts, the association with response to immunotherapy was tested using Fisher's exact test.

Results

Existing signatures showed no association with survival in stage I melanoma

The structure of datasets used in this study are depicted in Figure 1. When applied to the whole LMC dataset (n=687), the three formerly published signatures (Lund 4-class, Lund 2-grade, TCGA 3-class) replicated previously observed associations with MSS (Figure 2A, 2C, and 2E). However, upon stratifying LMC patients on the basis of AJCC stage, the Lund and TCGA signatures showed no association with prognosis for LMC stage I patients (Figure 2B, 2D, and 2F). The Lund 2-grade signature had the highest statistical power (since based on only two groups) and showed a statistically significant interaction with AJCC stage (P=0.02, Supplementary table S1), suggesting that the lack of association in stage I was not solely due to low sample size. Because the full details of Gerami *et al*'s (6) commercial signature were not published, we were limited in the scope of its replication in the LMC dataset. However, analysing the 27 Gerami genes identified 23 genes as

predictors of prognosis in the whole LMC dataset (Supplementary table S2). However, in keeping with the Lund and TCGA signatures, none of these genes showed a significant association with prognosis in stage I tumors (Supplementary table S2).

Generating novel LMC classes and their clinical characteristics

Consensus clustering of the LMC dataset was performed, and following additional quality control measures (Supplementary table S3), six distinct, novel molecular classes were identified (Figure 3A). These classes were associated with clinico-pathological variables known to have prognostic value, including tumor site (P=0.03), age at diagnosis (P=0.03), mitotic rate (P=0.002), ulceration (P=0.01), AJCC stage (P=6x10^{-10}), tumor infiltrating lymphocytes (TILs) (P=6x10^{-4}), and Breslow thickness (P=9x10^{-14}) (Table 1). The LMC classes 1 and 5 tumors tended to be thin and non-ulcerated, whilst classes 2 and 4 tumors were thicker. Class 3 and 6 tumors were the thickest and most frequently ulcerated. The six classes showed strong association with *BRAF* (P=6x10^{-5}) and *NRAS* mutation status (P=3x10^{-4}): classes 1, 5, and 6 tumors were frequently *BRAF* mutated, while classes 2, 3, and 4 tumors were frequently *NRAS* mutated (Table 1).

LMC classes predicted prognosis in primary melanoma and in stage I subset

The LMC classes predicted MSS in the whole LMC dataset and notably, across AJCC stages I, II and III subsets (Figure 3B-3C, Supplementary figure S1). In the unadjusted analysis of the whole dataset (Figure 3B, Supplementary table S4), class 1 (baseline) had the best prognosis, class 2 (HR=1.7, 95% confidence interval (CI) 0.8-3.5) and class 5 (HR=1.5, 95% CI 0.7- 3.1) showed intermediate prognosis, while class 3 (HR=5.0, 95% CI 2.5-10.1), class 4 (HR=2.4, 95% CI 1.2- 4.7), and class 6 (HR=3.1, 95% CI 1.6-6.1) had the worst prognosis. In multivariable analysis, classes 3, 4, and 6 remained significant predictors of poor prognosis after including AJCC stage, sex, age at diagnosis, mitotic rate (Table S4) and when the AJCC stage was replaced by ulceration and Breslow thickness in the model (Table S6). In the LMC stage I subset, class 6 (HR=6.6, 95% CI 1.4-31.2) significantly predicted poor prognosis in unadjusted analysis (Figure 3C and Table S5) and it remained significant

when sex, age at diagnosis, mitotic rate, ulceration and Breslow thickness were adjusted (HR=9.8, 95% CI 1.1-86.2, Table S6). Since Gerami signature was not available to us in full, we ran unsupervised clustering of the LMC dataset using the 27 Gerami genes to generate the 2 tumor groups analysed by Gerami *et al.* (6), referred to as the Gerami clusters. This analysis showed that the LMC classes and Gerami clusters had independent prognostic effects in the whole LMC dataset (Supplementary table S7); however, the Gerami clusters showed no prognostic value in stage I tumors while LMC class 6 remained a significant predictor in the multivariable model (Supplementary table S8).

To validate the prognostic value of the LMC classes in an independent dataset, a 150-gene based signature (LMC signature), generated after refining ~13,000 genes (Supplementary figure S2), was applied to the Lund dataset (4). In keeping with the observations made in the LMC dataset, class 3, class 4, and class 6 predicted worse prognosis in the Lund dataset, while class 1, class 2, and class 5 predicted better prognosis (Figure 3D, Supplementary table S9). Since the Lund dataset had only a few stage I cases (n=58) the prognostic value of LMC signature could not be replicated in stage I disease.

LMC signature had independent prognostic value when compared with SNB

In the dataset derived from individuals who had a SNB, the prognostic value of combined LMC class signature and pre-SNB AJCC stage was similar to that of AJCC stage with SNB (i.e. stage post-SNB) (AUC 0.82 vs 0.80, P= 0.7, Figure 3E). Combining the LMC signature with AJCC stage post-SNB, patient's sex, age at diagnosis and site of tumor increased the AUC to 0.88. Similarly, in the subset of patients at stage I pre-SNB, the LMC signature alone had comparable prognostic value to AJCC stage post-SNB (AUC=0.88 vs 0.83, P= 0.7, Figure 3F). In this stage I subset, addition of stage post-SNB, patient's sex, age at diagnosis and site of tumor to the LMC signature further increased the AUC to 0.98. However, the limited sample size of stage I dataset and including so many variables clearly overfitted the model, giving near perfect classification and illustrating that independent datasets are needed to better assess performance.

Biological overlap between the LMC and existing signatures

The six classes of LMC signature showed distinct gene expression profiles (Figure 4A) and showed partial overlap with the existing Lund and TCGA signatures. LMC classes 1, 3, and 5 overlapped substantially with the *high-immune*, *pigmentation,* and *normal-like* classes of the Lund 4-classes (Figure 4B), and with the *immune*, *MITF low,* and *keratin* classes of the TCGA 3-classes (Figure 4C). In contrast, LMC classes 2, 4, and 6 represented a mixture of the Lund 4-classes and TCGA 3-classes. Gene expression pathway enrichment analysis revealed distinctive biological features of the 6 LMC classes: notably class 2 was characterised by increased WNT signalling genes and metabolic pathways; class 4 by decreased expression of immune genes and class 6 by increased expression of cell cycle and consistent down-regulation of cell metabolism pathway genes (Supplementary table S14).

When applied to the LMC 6 classes, the Lund modules (29) revealed discrimination consistent with enriched gene pathways: LMC class 1 tumors showed higher *immune* module activity, and class 3 tumors showed higher *cell cycle* module activity (Figure 4D). Interestingly, class 6 tumors had relatively higher *cell cycle* but also *immune* module activity and, as expected, the *immune, stroma* and *interferon* modules were positively correlated but they negatively correlated with *cell cycle* and *MITF* modules (Figure 4D). The tumor infiltrating immune cell populations imputed for each of the LMC classes (30) were consistent with the Lund immune module, as class 1 had the highest immune cell populations and class 3 the lowest, whilst class 6 appeared to maintain an intermediate level of immune cell populations, having the second highest scores on average (Supplementary figure S3).

A comparison with the Consensus Immunome Clusters (CICs), previously generated in the same LMC dataset based on 380 immune genes (13), showed that the 2 most prognostically contrasted LMC classes (class 1 and class 3) had a near perfect match with CIC 2 (high Immune) and CIC 3 (low immune/β-catenin high) respectively (Supplementary figure S4) while the rest of LMC classes were a mixture of CICs. Cluster 1 had correspondingly a higher proportion of tumors with histological evidence of brisk tumor infiltrating lymphocytes (36% compared with 8% in class 3). Analysing the correlation between the Gerami genes and LMC signature genes showed that the Gerami genes positively correlated with the genes upregulated in LMC class 5 tumors and negatively correlated with

genes upregulated in LMC class 3 tumors (Supplementary figure S5). Consistent with this, Gerami clusters 1 and 2 highly overlapped with LMC classes 3 and 5 respectively (Supplementary figure S6).

JUN as marker of poor prognosis in class 6 tumors

LMC class 6 predicted worse prognosis within AJCC stage I tumors. Further biological network analysis identified *JUN* as a key upregulated nodal gene in this class (Figure 5A-B). The NGS-based CNA data from a subset of LMC tumors (*n*=272) indicated that class 6 tumors were more likely to have DNA amplifications of *JUN* than other classes (*P*=0.003, Figure 5C, Supplementary figure S7). In melanoma, *JUN* has been reported to activate epithelial-to-mesenchymal transition (EMT), and accordingly a 6-gene based (31) and 200-gene based EMT signature (32) consistently scored higher in LMC class 6 than in all other LMC classes (Figure 5D, Supplementary figure S7). A secondary key nodal gene *NFKB1* identified to be upregulated in class 6 had no copy number changes. Further examination of immunohistochemically stained sections, showed that all 4 tumors stained from class 6 were positive for NFKB1 protein expression, and this was similar to other LMC classes (P=0.4, Supplementary figure S7).

LMC signature as a potential predictor of response to immunotherapy

The value of the LMC signature in predicting outcome in patients treated with immunotherapy was assessed in three disparate clinical trial cohorts of metastatic melanoma (Figure 5F) (10-12). In the Hugo *et al*. cohort, tumors classified as class 6 were mainly non-responders to PD-1 blockade in comparison to the other LMC classes (*P*=0.03). Hugo *et al.* reported that expression of *AXL* predicts poor response to PD-1 blockade; the gene expression data revealed significantly higher *AXL* expression in class 6 tumors when compared to other classes within their cohort (Figure 5G). Similarly, for the cohort reported by Ulloa-Montoya *et al*., class 6 tumors showed a significantly higher proportion of non-responders to MAGE-A3 immunotherapy in comparison to other classes. The cohort reported by Riaz *et al.* was predominantly composed of non-responders to anti-CTLA-4 further treated with PD-1 blockade but LMC classes were not convincingly predictive but class 3 predicted poor

prognosis, which was consistent with the LMC dataset when compared to good prognosis class 1 (Figure 5H).

Discussion

In this study, transcriptome classification was performed utilising a large population-ascertained cohort of primary melanomas, revealing classes having prognostic value in stage I disease. In stage I tumors, the LMC signature predicted outcome comparably to AJCC staging including SNB. Furthermore, evidence suggests that the signature predicted outcome in patients treated with immunotherapies.

Given the rising incidence of early stage tumors and the cost of adjuvant therapies to health services and to patients in terms of toxicity, there is an urgent need to identify better prognostic and predictive biomarkers for early stage disease. When previous gene signatures were applied to the LMC (3,8), the signatures robustly predicted outcome when the dataset was analysed as a whole, but failed to do so in stage I tumors alone. Although the full Gerami signature was not available, analysing the prognostic value of genes reported in that study (6) showed that the genes were predictive of prognosis in the whole LMC dataset but not in stage I tumors. In this work, a six-class signature (Supplementary data file) was identified which was not only prognostic in the whole LMC dataset but also in patients diagnosed at AJCC stage I. The prognostic value of the LMC signature was validated in an independent cohort of primary melanoma built in Lund (4) although the number of stage I cases in this cohort was insufficient to allow replication of the signature's prognostic value in stage I disease.

The LMC signature showed limited overlap with the Lund and TCGA signatures. When comparing it with previously identified immunome clusters by our group (13), two LMC classes strongly overlapped with immune subgroups. The non-overlapping classes could not be clearly discriminated using the immunome clusters suggesting that these LMC classes are driven by different genomic mechanisms. Comparison of LMC signature genes with Gerami genes indicated a biological pathway overlap as Gerami genes were found to be strongly correlated with LMC classes 3 and 5.

Although SNB is an important melanoma staging tool, the surgery is associated with morbidity (33,34). In the LMC, SNB was observed to be of prognostic value in the whole dataset and in stage I

tumors. However, the LMC signature performed just as well. Given the morbidity of SNB, it may be argued that the LMC signature should be tested in an independent study as a possible alternative to this procedure especially in stage I disease where the likelihood of a positive result is overall low and must be weighed against morbidity.

In melanoma, increased immune gene expression has been consistently shown to predict good prognosis (5,9,13,35). However, a subset of tumors (LMC class 6) was observed which, despite showing immune gene expression, resulted in the patient's early death. Further biological characterisation of this class identified copy number amplifications and increased expression of *JUN*. Ramsdale *et al.* have shown that *JUN* promotes an invasive cell phenotype through activation of the EMT pathway (36), and a higher scoring EMT signature in LMC class 6 confirmed increased activity of the EMT pathway in this class. Riesenberg *et al.* have reported that increased *JUN* expression leads to pro-inflammatory and stress signals that promote cytokine expression in coordination with NF-κB (37). Again, these findings are consistent with the presented transcriptomic observations of *JUN* and *NFKB1* in defining LMC class 6 (Figure 5B, 5E). There was insufficient tissue to carry out immunohistochemistry for *JUN*, therefore *JUN* protein expression in the TCGA dataset was examined and confirmed a positive correlation between *JUN* gene transcription and protein expression (Supplementary figure S7). Collectively, these data are indicative of copy number gains resulting in both increased gene expression and transcriptional activity of *JUN* in LMC class 6 tumors, although further proteomic studies would be required to confirm this.

The LMC signature was associated with response to immunotherapies; specifically, class 6 associated with poor outcome in two of the three tested datasets. None of these data sets are sufficiently large to make clear inferences. It is of note that the expression of *AXL*, a known marker for immune evasion, was significantly upregulated in LMC class 6 in metastatic melanoma samples in the Hugo data set.

The inherent strength of this study is the relatively large size of the population ascertained cohort. A corresponding limitation is the lack of a well powered AJCC stage I dataset to allow independent replication of the signature in stage I melanoma. Another limitation of this study is that only one-third of LMC patients had a SNB, limiting the power to compare staging tests. The LMC recruitment period preceded the advent of both immunotherapy and targeted therapy, and only a very small number of the study participants have been treated with these drugs. Excluding the samples from these

participants showed no modifying effect of such treatments on MSS in the LMC dataset (data not shown).

In conclusion, this study presents a novel signature with demonstrated prognostic value similar in magnitude to that of AJCC staging of melanoma, but having added value in stage I melanoma. The data further confirm that AJCC stage largely captures biological variation associated with survival. The LMC class signature prognostic value was similar to that of SNB in the whole dataset (where their effects were additive) and in stage I disease. The signature predicted poor outcome in patients receiving immunotherapies and in particular identified high-*JUN*/high-*AXL* as a tumor phenotype with poor prognosis in early and advanced stage melanoma albeit in very small datasets. This signature has the potential to be trialled as a biomarker in clinical monitoring programs and may help in early identification of patients who may or may not benefit from adjuvant therapies.

Acknowledgements

We thank all the participants of the LMC study and the research nurses who conducted the recruitment.

Accession number

The accession number for the microarray data reported in this paper is European Genome Archive accession number: EGAS00001002922.

References

1. Lo SN, Scolyer RA, Thompson JF. Long-term survival of patients with thin (T1) cutaneous melanomas: a Breslow thickness cut point of 0.8 mm separates higher-risk and lower-risk tumors. Annals of surgical oncology **2018**;25(4):894-902.
2. Cancer research UK 21st September 2018. https://www.cancerresearchuk.org/health-professional/cancer-statistics/statistics-by-cancer-type/melanoma-skin-cancer/diagnosis-and-treatment#ref-1.

3. Jonsson G, Busch C, Knappskog S, Geisler J, Miletic H, Ringner M*, et al.* Gene expression profiling-based identification of molecular subtypes in stage IV melanomas with different clinical outcome. Clin Cancer Res **2010**;16(13):3356-67 doi 10.1158/1078-0432.CCR-09-2509.

4. Harbst K, Staaf J, Lauss M, Karlsson A, Masback A, Johansson I*, et al.* Molecular profiling reveals low- and high-grade forms of primary melanoma. Clin Cancer Res **2012**;18(15):4026-36 doi 10.1158/1078-0432.CCR-12-0343.

5. Nsengimana J, Laye J, Filia A, Walker C, Jewell R, Van den Oord JJ*, et al.* Independent replication of a melanoma subtype gene signature and evaluation of its prognostic value and biological correlates in a population cohort. Oncotarget **2015**;6(13):11683-93 doi 10.18632/oncotarget.3549.

6. Gerami P, Cook RW, Wilkinson J, Russell MC, Dhillon N, Amaria RN*, et al.* Development of a prognostic genetic signature to predict the metastatic risk associated with cutaneous melanoma. Clin Cancer Res **2015**;21(1):175-83 doi 10.1158/1078-0432.CCR-13-3316.

7. Ferris LK, Farberg AS, Middlebrook B, Johnson CE, Lassen N, Oelschlager KM*, et al.* Identification of high-risk cutaneous melanoma tumors is improved when combining the online American Joint Committee on Cancer Individualized Melanoma Patient Outcome Prediction Tool with a 31-gene expression profile–based classification. Journal of the American Academy of Dermatology **2017**;76(5):818-25. e3.

8. The Cancer Genome Atlas Network. Genomic classification of cutaneous melanoma. Cell **2015**;161(7):1681-96.

9. Lauss M, Nsengimana J, Staaf J, Newton-Bishop J, Jonsson G. Consensus of Melanoma Gene Expression Subtypes Converges on Biological Entities. J Invest Dermatol **2016**;136(12):2502-5 doi 10.1016/j.jid.2016.05.119.

10. Hugo W, Zaretsky JM, Sun L, Song C, Moreno BH, Hu-Lieskovan S*, et al.* Genomic and Transcriptomic Features of Response to Anti-PD-1 Therapy in Metastatic Melanoma. Cell **2016**;165(1):35-44 doi 10.1016/j.cell.2016.02.065.

11. Ulloa-Montoya F, Louahed J, Dizier B, Gruselle O, Spiessens B, Lehmann FF*, et al.* Predictive gene signature in MAGE-A3 antigen-specific cancer immunotherapy. J Clin Oncol **2013**;31(19):2388-95 doi 10.1200/JCO.2012.44.3762.

12. Riaz N, Havel JJ, Makarov V, Desrichard A, Urba WJ, Sims JS*, et al.* Tumor and Microenvironment Evolution during Immunotherapy with Nivolumab. Cell **2017**;171(4):934-49 e16 doi 10.1016/j.cell.2017.09.028.

13. Nsengimana J, Laye J, Filia A, O'Shea S, Muralidhar S, Pozniak J*, et al.* beta-Catenin-mediated immune evasion pathway frequently operates in primary cutaneous melanomas. J Clin Invest **2018**;128(5):2048-63 doi 10.1172/JCI95351.

14. Clark Jr WH, Elder DE, Guerry IV D, Braitman LE, Trock BJ, Schultz D*, et al.* Model predicting survival in stage I melanoma based on tumor progression. JNCI: Journal of the National Cancer Institute **1989**;81(24):1893-904.

15. Gershenwald JE, Scolyer RA. Melanoma Staging: American Joint Committee on Cancer (AJCC) 8th Edition and Beyond. Annals of Surgical Oncology **2018**;25(8):2105-10 doi 10.1245/s10434-018-6513-7.

16. Du P, Kibbe WA, Lin SM. lumi: a pipeline for processing Illumina microarray. Bioinformatics **2008**;24(13):1547-8 doi 10.1093/bioinformatics/btn224.

17. Lauss M, Visne I, Kriegner A, Ringner M, Jonsson G, Hoglund M. Monitoring of technical variation in quantitative high-throughput datasets. Cancer Inform **2013**;12:193-201 doi 10.4137/CIN.S12862.

18. Wilkerson MD, Hayes DN. ConsensusClusterPlus: a class discovery tool with confidence assessments and item tracking. Bioinformatics **2010**;26(12):1572-3 doi 10.1093/bioinformatics/btq170.

19. Monti S, Tamayo P, Mesirov J, Golub T. Consensus clustering: a resampling-based method for class discovery and visualization of gene expression microarray data. Machine learning **2003**;52(1-2):91-118.

20. Therneau TM, Lumley T. Package 'survival'. Verze; 2017.

458 21. Robin X, Turck N, Hainard A, Tiberti N, Lisacek F, Sanchez JC*, et al.* pROC: an open-source
459 package for R and S+ to analyze and compare ROC curves. BMC Bioinformatics **2011**;12(1):77
460 doi 10.1186/1471-2105-12-77.

461 22. Sachs M. plotROC: Generate Useful ROC Curve Charts for Print and Interactive Use, 2016. URL
462 http://sachsmcgithubio/plotROC R package version;2(1):220.

463 23. Wickham H. ggplot2: elegant graphics for data analysis. Springer; 2016.

464 24. Tibshirani R, Chu G, Narasimhan B, Li J. samr: SAM: Significance Analysis of Microarrays. R
465 package version 2.0. 2011.

466 25. Wu G, Dawson E, Duong A, Haw R, Stein L. ReactomeFIViz: a Cytoscape app for pathway and
467 network-based data analysis. F1000Res **2014**;3:146 doi 10.12688/f1000research.4431.2.

468 26. Bastian M, Heymann S, Jacomy M. Gephi: an open source software for exploring and
469 manipulating networks. Icwsm **2009**;8:361-2.

470 27. Durinck S, Moreau Y, Kasprzyk A, Davis S, De Moor B, Brazma A*, et al.* BioMart and
471 Bioconductor: a powerful link between biological databases and microarray data analysis.
472 Bioinformatics **2005**;21(16):3439-40.

473 28. Durinck S, Spellman PT, Birney E, Huber W. Mapping identifiers for the integration of genomic
474 datasets with the R/Bioconductor package biomaRt. Nat Protoc **2009**;4(8):1184-91 doi
475 10.1038/nprot.2009.97.

476 29. Cirenajwis H, Ekedahl H, Lauss M, Harbst K, Carneiro A, Enoksson J*, et al.* Molecular
477 stratification of metastatic melanoma using gene expression profiling: Prediction of survival
478 outcome and benefit from molecular targeted therapy. Oncotarget **2015**;6(14):12297.

479 30. Angelova M, Charoentong P, Hackl H, Fischer ML, Snajder R, Krogsdam AM*, et al.*
480 Characterization of the immunophenotypes and antigenomes of colorectal cancers reveals
481 distinct tumor escape mechanisms and novel targets for immunotherapy. Genome Biol
482 **2015**;16(1):64 doi 10.1186/s13059-015-0620-6.

483 31. Huang RY, Kuay KT, Tan TZ, Asad M, Tang HM, Ng AH*, et al.* Functional relevance of a six
484 mesenchymal gene signature in epithelial-mesenchymal transition (EMT) reversal by the triple

angiokinase inhibitor, nintedanib (BIBF1120). Oncotarget **2015**;6(26):22098-113 doi 10.18632/oncotarget.4300.

32. Liberzon A, Birger C, Thorvaldsdottir H, Ghandi M, Mesirov JP, Tamayo P. The Molecular Signatures Database (MSigDB) hallmark gene set collection. Cell Syst **2015**;1(6):417-25 doi 10.1016/j.cels.2015.12.004.

33. Balch CM, Gershenwald JE, Soong SJ, Thompson JF, Atkins MB, Byrd DR*, et al.* Final version of 2009 AJCC melanoma staging and classification. J Clin Oncol **2009**;27(36):6199-206 doi 10.1200/JCO.2009.23.4799.

34. Morton DL, Cochran AJ, Thompson JF, Elashoff R, Essner R, Glass EC*, et al.* Sentinel node biopsy for early-stage melanoma: accuracy and morbidity in MSLT-I, an international multicenter trial. Ann Surg **2005**;242(3):302-11; discussion 11-3.

35. Lauss M, Donia M, Harbst K, Andersen R, Mitra S, Rosengren F*, et al.* Mutational and putative neoantigen load predict clinical benefit of adoptive T cell therapy in melanoma. Nat Commun **2017**;8(1):1738 doi 10.1038/s41467-017-01460-0.

36. Ramsdale R, Jorissen RN, Li FZ, Al-Obaidi S, Ward T, Sheppard KE*, et al.* The transcription cofactor c-JUN mediates phenotype switching and BRAF inhibitor resistance in melanoma. Sci Signal **2015**;8(390):ra82 doi 10.1126/scisignal.aab1111.

37. Riesenberg S, Groetchen A, Siddaway R, Bald T, Reinhardt J, Smorra D*, et al.* MITF and c-Jun antagonism interconnects melanoma dedifferentiation with pro-inflammatory cytokine responsiveness and myeloid cell recruitment. Nature communications **2015**;6:8755.

Table 1 The LMC classes association with clinico-histopathological variables

Histopathological variables	Whole dataset *n*=687 (%)	LMC classes						
		Class 1 (*n*=71)	Class 2 (*n*=122)	Class 3 (*n*= 73)	Class 4 (*n*=143)	Class 5 (*n*=136)	Class 6 (*n*=142)	P[a]
Sex : male *n* (%)	310 (45)	39 (55)	51 (42)	34 (47)	56 (39)	55 (40)	75 (52)	0.07
Tumor site: limbs *n* (%)	289 (42)	37 (52)	58 (48)	26 (36)	58 (41)	64 (47)	46 (32)	0.03
Age at diagnosis (years) m(r)	58 (18, 81)	59 (21,76)	59 (22,79)	60 (20,77)	58 (18,81)	53 (25,76)	59 (22,81)	0.03
Breslow thickness (mm) m(r)	2.3 (0.3, 20)	1.7 (0.7, 5.5)	2.1 (0.8, 8.9)	3.2 (0.8, 20)	2.3 (0.3, 15)	1.8 (0.7, 12)	3.0 (0.8, 18)	9×10^{-14}
AJCC stage (%) [b] I **II** **III**	236 (35) 335 (49) 109 (16)	39 (55) 26 (36) 6 (9)	42 (35) 57 (48) 21 (17)	11 (15) 46 (64) 15 (21)	46 (33) 77 (55) 18 (12)	71 (53) 45 (33) 19 (14)	27 (19) 84 (60) 30 (21)	6×10^{-10}
Ulceration (present) *n* (%)	228 (33)	16 (23)	32 (26)	30 (41)	53 (37)	38 (28)	59 (42)	0.01
Mitotic rate (/mm^2)	1 (0,25)	0 (0,11)	1 (0,17)	2 (0,25)	1 (0,13)	1 (0,12)	1 (0,18)	0.002
TILs (%) Absent **Non-Brisk** **Brisk**	76 (15) 333 (68) 81 (17)	2 (4) 30 (60) 18 (36)	13 (14) 65 (71) 14 (15)	17 (32) 32 (60) 4 (8)	14 (16) 60 (68) 14 (16)	15 (16) 63 (66) 17 (18)	15 (13) 83 (74) 14 (13)	6×10^{-4}
***BRAF* mutant yes (%)**	266 (47)	26 (43)	38 (30)	23 (40)	44 (36)	63 (59)	72 (61)	6×10^{-5}
***NRAS* mutant yes (%)**	138 (25)	8 (14)	35 (34)	17 (30)	41 (34)	20 (19)	17 (15)	3×10^{-4}

[a]The associations were tested using Pearson's chi-squared test for categorical variables and the Kruskal-Wallis test for continuous variables. Symbol *n* is the number of samples, *m* is the median and *r* is the range. [b] 7 patients had mucosal melanoma and, although they were classified, they were not included in survival analyses. Their AJCC stage was not reported. Each of LMC class 2 and 4 contained 2 of these, while class 3, 5 and 6 had 1 each.

Figure legends

Figure 1: Analysis workflow of the study

Figure 2: Replicating Lund and TCGA signatures using LMC dataset. Kaplan-Meier plots showing the Melanoma-specific survival (MSS) for (A) Lund 4-classes (HI- *high-immune*, NL- *normal-like*, Pigm.- *pigmentation*, Prolif.- *proliferative*), (B) Lund 2-grades (*low grade* and *high grade*) and (C) TCGA 3-classes (*immune*, *keratin*, *MITF low*) across the whole LMC dataset. In LMC stage I subset, Kaplan-Meier plots showing the MSS for (D) Lund 4-classes, (E) Lund 2-grades, and (F) TCGA 3-classes. Pvalues are from log-rank test. Samples which could not be classified into any of the classes were not used in survival analysis.

Figure 3: Defining LMC signature and its prognostic value. (A) The area under the CDF and its relative change with increasing *k*. The delta area graph shows little variation at *k*=6. Heatmap of consensus matrices at *k*=5 and 6. The blue color indicates high consensus score and the white color indicates low consensus (B) Kaplan-Meier plot showing the MSS for the six classes in (B) the whole LMC dataset, (C) the LMC stage I, and (D) relapse-free survival in the Lund cohort (Pvalue from log-rank test, or Wald test for two-groups comparison). Seven mucosal tumors were excluded from analysis. (E) ROC curves comparing the prognostic value of the LMC signature to that of Sentinel Node Biopsy (SNB) in the whole dataset. The AUCs for LMC class+ stage pre-SNB and stage post-SNB were not significantly different (DeLong's test P=0.7). (F) The ROC curve comparing prognostic value of LMC signature with SNB in the stage I pre-SNB group. All but one patient were stage IB pre-SNB, therefore AUC for LMC signature alone was compared to stage post-SNB and the difference was not significant (DeLong's test P=0.7). The difference in AUCs between stage post-SNB alone and LMC class +stage post-SNB was also not significant (DeLong's test P=0.1).

Figure 4: Biological characterization of the six LMC classes. (A) The heatmap shows gene expression across the classes with tumor samples placed in columns and genes in rows. Blue depicts low expression and red depicts high expression. Each gene expression was standardized to mean 0 and

standard deviation 1. The up- and down-regulated nodal genes identified in network analyses are shown under the heatmap. The barplot shows the overlap between the LMC classes and (B) Lund 4-classes (HI- *high-immune*, NL- *normal-like*, Pigm- *pigmentation*, Prolif- *proliferative*), and (C) TCGA 3-classes. The samples that could not be classified into the Lund 4-classes and TCGA 3-classes were labelled here as *Uncls.* (D) The modules (defined by a list of differentially upregulated genes) associated with melanoma-specific biological pathways as identified by the Lund group (29). Boxplots of *immune and cell cycle* module scores (standardized expressions) within the 6 LMC classes and correlation matrix of *immune, cell cycle, MITF, stroma and interferon module scores*. The module score variation across the classes was tested using the Kruskal-Wallis test.

Figure 5: Biological characterization of LMC class 6 and association with response to immunotherapy. (A) Network of upregulated genes in the LMC class 6 with key genes (highest betweenness centrality) shown as large circles. Sub-networks are shown in different colors. (B) Expression of *JUN* across the six LMC classes (Pvalue from Kruskal-Wallis test). (C) *JUN* copy number alterations in *LMC* class 6 *vs* other classes. (D) The 6-gene based EMT score in tumors across the six LMC classes (Pvalue from Kruskal-Wallis test). (E) The gene expression of *NFKB1* across the 6 LMC classes (Pvalue from Kruskal-Wallis test). (F) The LMC classes association with response to immunotherapy in three cohorts (Pvalue from Fisher's exact test). Patients in these cohorts were classified into the 6 LMC classes by the NCC method. (G) Expression of *AXL* across the six LMC classes in the Hugo Cohort dataset (Pvalue from Mann–Whitney U test). (H) Kaplan-Meier plot showing survival curves of LMC class 1, class 3, and class 6 in the Riaz Cohort. Other LMC classes had <5 samples and were excluded.

562 **Figure 1**

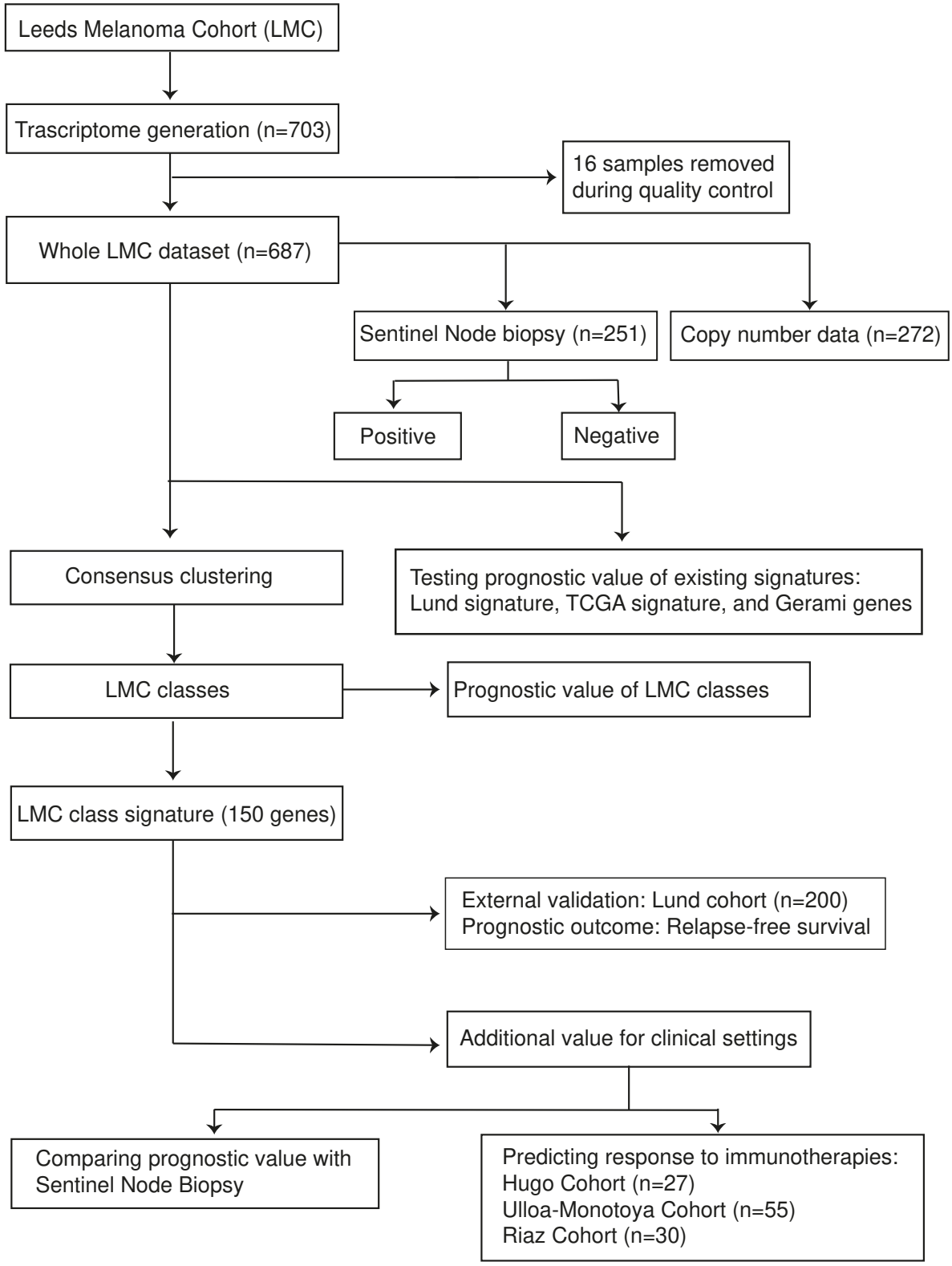

563

564

Figure 2

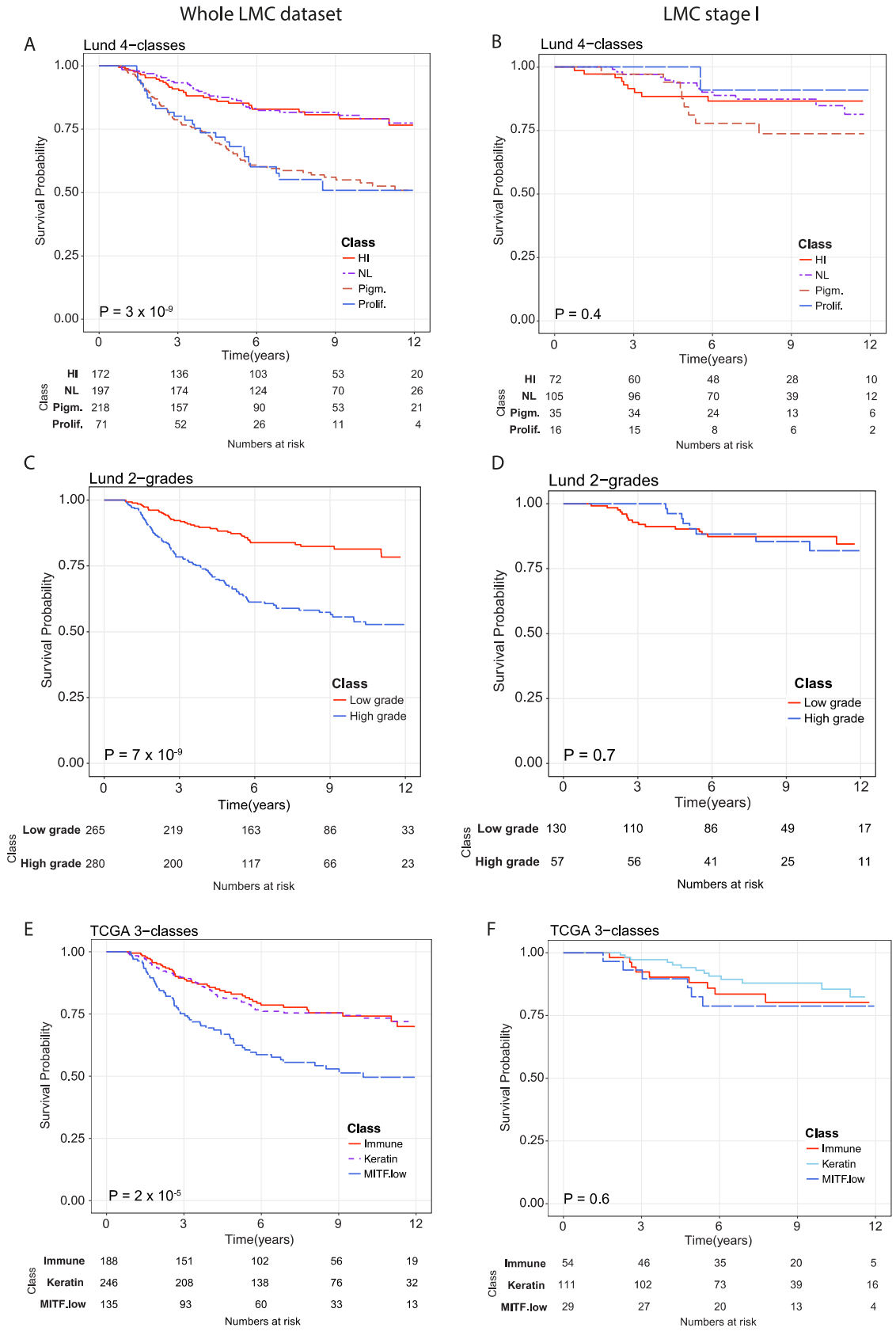
Whole LMC dataset
LMC stage I
A
Lund 4−classes
Survival Probability
Time(years)
Class
HI
NL
Pigm.
Prolif.
P = 3 x 10-9
HI 172 136 103 53 20
NL 197 174 124 70 26
Pigm. 218 157 90 53 21
Prolif. 71 52 26 11 4
Numbers at risk
B
Lund 4−classes
P = 0.4
HI 72 60 48 28 10
NL 105 96 70 39 12
Pigm. 35 34 24 13 6
Prolif. 16 15 8 6 2
Numbers at risk
C
Lund 2−grades
Low grade
High grade
P = 7 x 10-9
Low grade 265 219 163 86 33
High grade 280 200 117 66 23
Numbers at risk
D
Lund 2−grades
P = 0.7
Low grade 130 110 86 49 17
High grade 57 56 41 25 11
Numbers at risk
E
TCGA 3−classes
Immune
Keratin
MITF.low
P = 2 x 10-5
Immune 188 151 102 56 19
Keratin 246 208 138 76 32
MITF.low 135 93 60 33 13
Numbers at risk
F
TCGA 3−classes
P = 0.6
Immune 54 46 35 20 5
Keratin 111 102 73 39 16
MITF.low 29 27 20 13 4
Numbers at risk

Figure 3

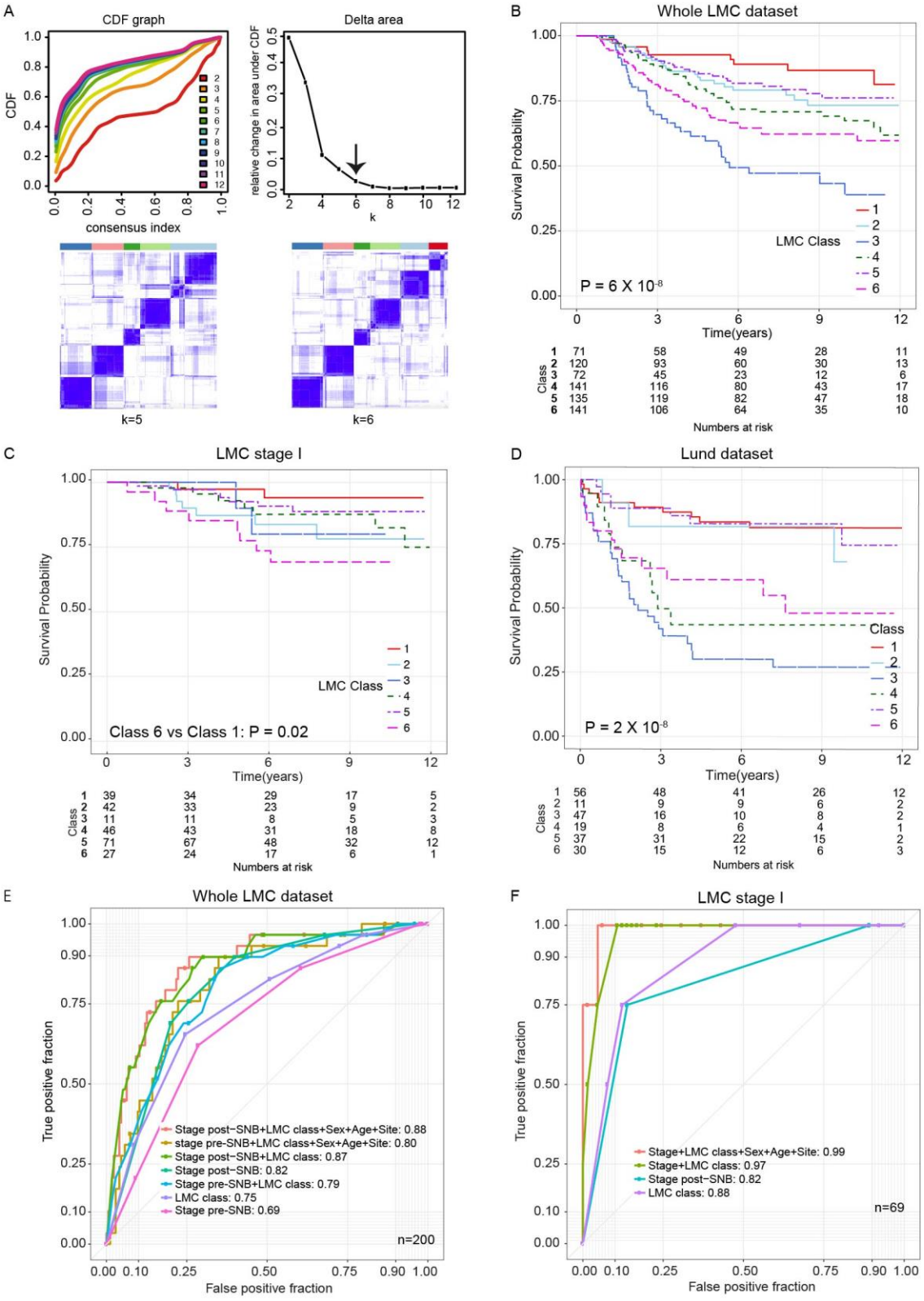
A
CDF graph
CDF
consensus index
Delta area
relative change in area under CDF
k
k=5
k=6
B
Whole LMC dataset
Survival Probability
LMC Class
P = 6 X 10-8
Time(years)
Class
Numbers at risk
C
LMC stage I
Class 6 vs Class 1: P = 0.02
D
Lund dataset
P = 2 X 10-8
E
Whole LMC dataset
True positive fraction
False positive fraction
Stage post−SNB+LMC class+Sex+Age+Site: 0.88
stage pre-SNB+LMC class+Sex+Age+Site: 0.80
Stage post−SNB+LMC class: 0.87
Stage post−SNB: 0.82
Stage pre-SNB+LMC class: 0.79
LMC class: 0.75
Stage pre-SNB: 0.69
n=200
F
LMC stage I
Stage+LMC class+Sex+Age+Site: 0.99
Stage+LMC class: 0.97
Stage post−SNB: 0.82
LMC class: 0.88
n=69

Figure 4

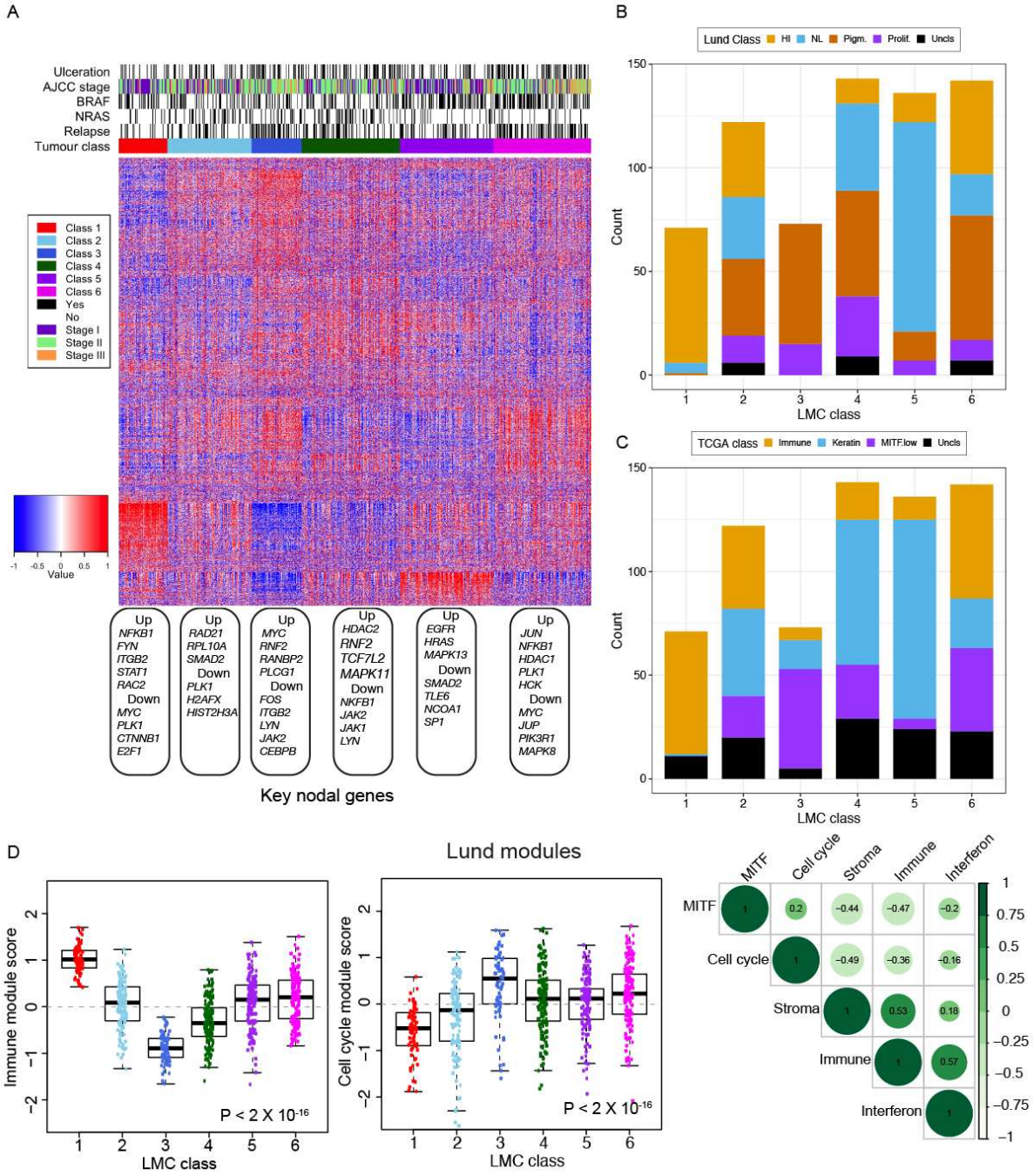
A
Ulceration
AJCC stage
BRAF
NRAS
Relapse
Tumour class
Class 1
Class 2
Class 3
Class 4
Class 5
Class 6
Yes
No
Stage I
Stage II
Stage III
Value
Up
NFKB1
FYN
ITGB2
STAT1
RAC2
Down
MYC
PLK1
CTNNB1
E2F1
Up
RAD21
RPL10A
SMAD2
Down
PLK1
H2AFX
HIST2H3A
Up
MYC
RNF2
RANBP2
PLCG1
Down
FOS
ITGB2
LYN
JAK2
CEBPB
Up
HDAC2
RNF2
TCF7L2
MAPK11
Down
NKFB1
JAK2
JAK1
LYN
Up
EGFR
HRAS
MAPK13
Down
SMAD2
TLE6
NCOA1
SP1
Up
JUN
NFKB1
HDAC1
PLK1
HCK
Down
MYC
JUP
PIK3R1
MAPK8
Key nodal genes
B
Lund Class HI NL Pigm. Prolif. Uncls
Count
LMC class
C
TCGA class Immune Keratin MITF.low Uncls
Count
LMC class
D
Lund modules
Immune module score
P < 2 X 10-16
LMC class
Cell cycle module score
P < 2 X 10-16
LMC class
MITF
Cell cycle
Stroma
Immune
Interferon
1
0.75
0.5
0.25
0
−0.25
−0.5
−0.75
−1

Figure 5

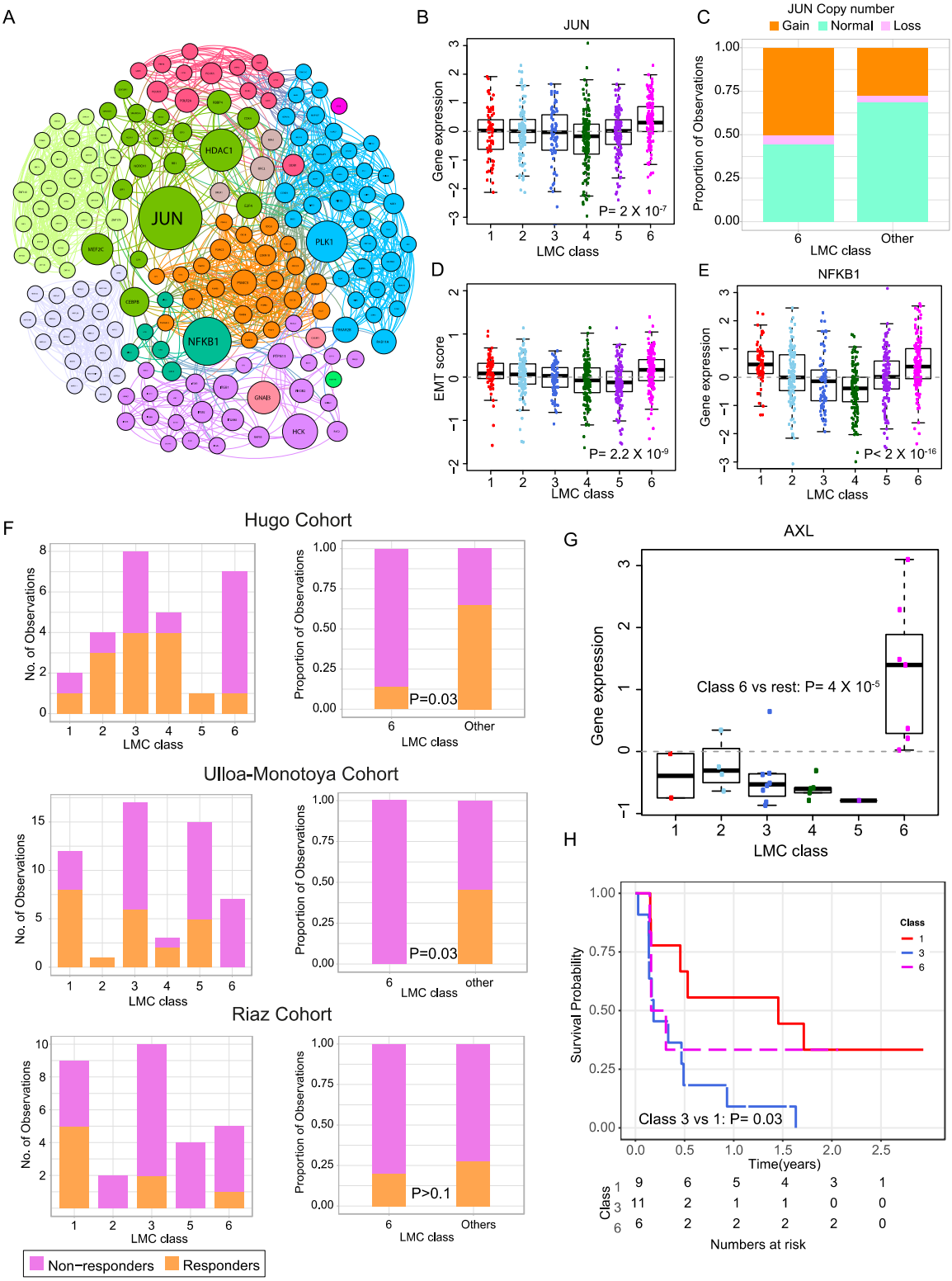
A
HDAC1
JUN
PLK1
NFKB1
HCK
B
JUN
Gene expression
P= 2 X 10-7
LMC class
C
JUN Copy number
Gain
Normal
Loss
Proportion of Observations
6
Other
LMC class
D
EMT score
P= 2.2 X 10-9
LMC class
E
NFKB1
Gene expression
P< 2 X 10-16
LMC class
F
Hugo Cohort
No. of Observations
LMC class
Proportion of Observations
P=0.03
6
Other
LMC class
Ulloa-Monotoya Cohort
No. of Observations
LMC class
Proportion of Observations
P=0.03
6
other
LMC class
Riaz Cohort
No. of Observations
LMC class
Proportion of Observations
P>0.1
6
Others
LMC class
Non−responders
Responders
G
AXL
Gene expression
Class 6 vs rest: P= 4 X 10-5
LMC class
H
Survival Probability
Class
1
3
6
Class 3 vs 1: P= 0.03
Time(years)
Class
1 9 6 5 4 3 1
3 11 2 1 1 0 0
6 6 2 2 2 2 0
Numbers at risk